PNAS RESEARCH ARTICLE | MICROBIOLOGY

HCV NS3/4A protease relocalizes CCTα to viral replication sites, enhancing phosphatidylcholine synthesis and viral replication

Shamila Sarwar[a] and Glenn Randall[a,1]

Edited by Peter Sarnow, Stanford University School of Medicine, Stanford, CA; received September 25, 2024; accepted January 28, 2025

Positive-sense single-stranded RNA [(+)RNA] viruses constitute more than one-third of all virus genera, including numerous pathogens of clinical significance. All (+)RNA viruses reorganize cellular membranes from organelles to establish replication compartments (RCs). These RCs are thought to form a platform for membrane-associated replicases, in addition to protecting the viral RNAs from cytosolic innate immune signaling and RNA-degradation machinery. Previous work demonstrated that three families of (+)RNA viruses, namely *Bromoviridae*, *Picornaviridae*, and *Flaviviridae*, commonly induce the accumulation of phosphatidylcholine (PC) at their RCs. This phenomenon suggests a potential avenue for a broad-spectrum antiviral strategy targeting PC metabolism. Our study elucidates three key observations: i) hepatitis C virus (HCV) infection prompts the relocalization of CCTα, the rate-limiting enzyme in PC synthesis, to the RCs; ii) the enhancement of PC synthesis is contingent upon the protease activity of the NS3/4A protein; and iii) utilizing click chemistry, we demonstrate that HCV infection stimulates de novo PC synthesis at the viral replication site through the Kennedy pathway. These findings provide significant insights into the manipulation of lipid metabolism by HCV during RC formation, a mechanism likely conserved across various (+)RNA virus families.

viral replication compartments | viral proteases | lipid synthesis

Significance

Like all (+)RNA viruses, HCV modifies the cytosolic membrane of infected cells to establish RCs. Multiple (+)RNA viruses induce PC accumulation at RCs. We find that HCV infection induces de novo PC synthesis at the viral replicating site. HCV infection and expression of NS3/4A result in the relocalization of the rate-limiting enzyme CCTα, from the nucleus, where it is inactive, to viral RCs, suggesting the role of the Kennedy pathway in HCV-specific PC synthesis. This study connects the HCV protease to modulation of the Kennedy pathway to stimulate PC synthesis localized to RCs. It also highlights the Kennedy pathway as a potential broad-spectrum antiviral therapeutic target.

Chronic hepatitis C virus (HCV) infection causes serious life-threatening liver diseases like cirrhosis and hepatocellular carcinoma (1). Despite effective antivirals, 1.75 million new HCV infections and 400,00 related deaths occur annually, and an estimated 51 million people are living with chronic HCV infection worldwide (2, 3). Chronic HCV infections are also often associated with hyperlipidemia, one of the major risk factors of cardiovascular diseases (4, 5). Thus, HCV infection is a major socioeconomic burden to our society.

HCV, the causative agent of chronic HCV infection, is a positive-strand RNA virus of the family *Flaviviridae*. Positive-strand RNA viruses are well known for remodeling the host intracellular membranes to form replication compartments (RCs) (6). These RCs provide a platform for membrane-associated replicases and protect viral RNAs from cytosolic innate immune signaling and RNA-degradation machinery (7). RNA replication of Dengue virus (8) or West Nile virus (9) occurs within the ER membrane invaginations, and that of Flock House virus (FHV) (10) and Semliki Forest virus (11, 12) takes place on the outer mitochondrial membrane and the plasma membrane, respectively. In contrast, HCV proteins induce ER membrane rearrangement eventually forming heterogeneous membranous vesicles that resembles membranous web (13). Though all positive-strand RNA virus shares a common feature of membrane rearrangement, they differ in the origin and the biogenesis of these compartments.

HCV encodes a polyprotein inside the cells, which is co-, and posttranslationally cleaved by cellular and viral protease into four structural (core, E1, E2, and p7) and six nonstructural proteins (NS2, NS3, NS4A, NS4B, NS5A, and NS5B). The 3D architecture of the HCV-induced membranous web appears to consist of single membrane vesicles (SMV) and double-membrane vesicles (DMV). The DMVs are thought to represent the functional RC and are a shared property of many (+)RNA viruses (14). The ectopic expression of individual HCV proteins suggests that NS3/4A can induced complex large SMVs, NS4B induced smaller and more homogenous SMVs, NS5A can form DMVs and multiple-membrane vesicles (MMVs) while NS5B expressing cells shows some ER invaginations (15). Thus, formation of membranous web is a concerted action of viral NS3-5B proteins (16).

Our lab and others have shown that a key component in the viral mechanism of RC formation is the modulation of RC membrane lipid composition (17). In the case of the HCV, the NS5A protein binds to and activates a cellular phosphatidyl inositol (PI) kinase, which then recruits lipid transfer proteins to modify the ER cholesterol content (18–20). While this mechanism is critical for HCV replication, we are beginning to appreciate

Author affiliations: [a]Department of Microbiology, The University of Chicago, Chicago, IL 60637

Author contributions: S.S. and G.R. designed research; S.S. performed research; S.S. analyzed data; and S.S. and G.R. wrote the paper.

The authors declare no competing interest.

This article is a PNAS Direct Submission.

[1]To whom correspondence may be addressed. Email: grandall@bsd.uchicago.edu.

Published March 5, 2025.

that it is also far from a complete description of viral alterations in lipid metabolism. Several studies have shown that HCV infection perturbs host lipid biosynthetic pathways (21). Shotgun lipidomic analysis indicated an increase in membrane lipids, especially phosphatidylcholine (PC), phosphatidylethanolamine (PE), and phosphatidylinositol (PI) levels in the microsomal fraction of HCV-infected cells (22). Additionally, one study using a metabolomic-based approach highlights elevated levels of phosphatidylinositol and phosphocholine-based lysophospholipids (LPLs) in HCV-infected hepatocytes (23). Also, in collaboration with Wang lab, we previously published that (+)RNA viruses such as BMV, poliovirus, and HCV share the property of stimulating PC synthesis/ accumulation at RCs (24). This suggests that understanding viral modulation of PC synthesis may have broad implication as a conserved mechanism in RC formation. We have extended this observation in HCV to gain significant mechanistic insight into this process.

PC constitutes half of the total phospholipid content of eukaryotic host cell and subcellular organelle membranes (25). In eukaryotes, PC is synthesized via the cytidine diphosphate-diacylglycerol (CDP-DAG) and Kennedy pathways, the latter responsible for 70% PC production in mammalian liver cells (26). There are several reports supporting the elevated level of PC during HCV infection, but the exact significance and the mechanism of HCV infection–specific activation of PC synthesis are still to be determined. Besides, PC is also a precursor for the biosynthesis of lipid signaling molecules and thus of utmost importance to understand host–HCV interaction better. In this article, we use click chemistry to show that HCV infection induces de novo synthesis of PC at the viral replication site via the Kennedy pathway. Our study also reveals that HCV NS3-4A protease orchestrates relocalization of CTP-phosphocholine-cytidyl transferase alpha (CCTα) from the nuclei of infected cells to viral RCs, stimulating PC synthesis. This broadly expands our appreciation of potential roles for viral proteases during replication.

Results

HCV Infection Induces De Novo PC Synthesis. Previously, we demonstrated that PC accumulates at the HCV RC, using immunostaining with anti-PC antibody (JE-1) (23). This observation motivated us to check whether there is de novo synthesis of PC at the site of HCV replication. To do so, we metabolically pulse-labeled the de novo synthesized PC with propargylcholine, a choline analog consisting of a terminal alkyne moiety (Fig. 1*B*). The incorporated propargylcholine can then be covalently linked with a fluorescent- (Alexa 488) labeled azide via click chemistry (Fig. 1*C*) (27–29). Briefly, we imaged newly synthesized PC in HCV-infected Huh7.5 cells by culturing the cells with 100 μM propargylcholine for 1 h in serum-free media, followed by fixation and labeling with click reaction. Quantification of PC fluorescent intensity suggested that HCV infection significantly stimulated PC synthesis by approximately 2.5-fold per cell (Fig. 1 *D* and *E*). Furthermore, the PC signal was found to be diffused throughout the cellular membranes in mock-infected cells, whereas in HCV-infected cells, the PC signal was concentrated in the perinuclear region and colocalized with the HCV NS5A protein (Fig. 1*F*).

HCV Modulates the Cellular Kennedy Pathway to Stimulate PC Synthesis. The majority of PC is synthesized in the liver via the Kennedy pathway. CCTα catalyzes the rate-limiting step in the pathway and shuttles between the nucleus and cytosol depending on the status of membrane biogenesis (30, 31). To understand the involvement of the Kennedy pathway in HCV-induced PC synthesis, we characterized the localization pattern of CCTα. Under normal physiological conditions, CCTα shuttles between a predominant nuclear and a less abundant cytosolic pool. When cells proliferate and require PC for membrane biogenesis, CCTα relocates from the nucleus (in soluble form) to a perinuclear/ER membrane (in membrane-bound form) and becomes activated (32, 33). Huh 7.5 cells were infected with HCV for 18 h, then fixed and

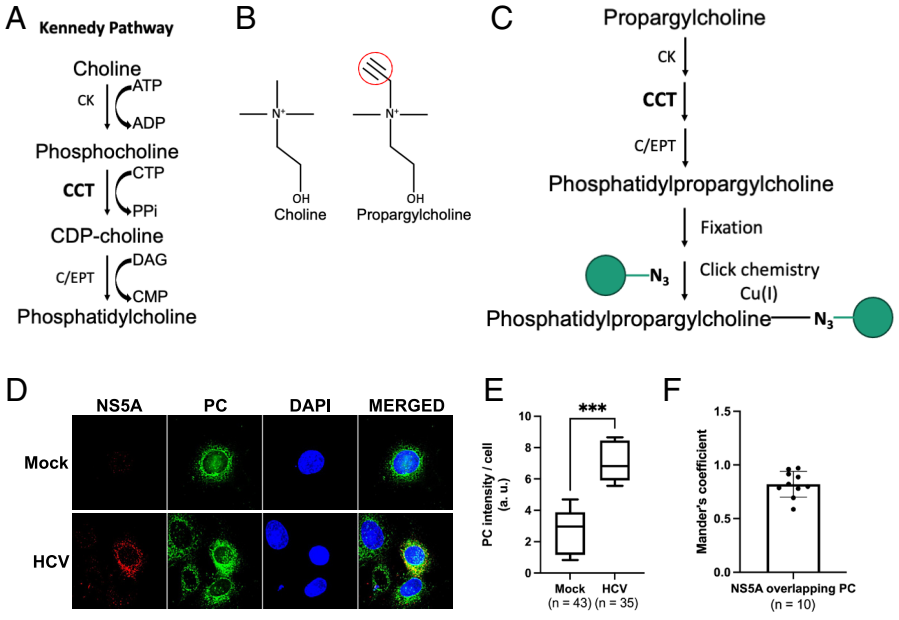

Fig. 1. HCV infection induces PC synthesis at the viral replication site. (*A*) Schematic representation of the Kennedy pathway. (*B*) Chemical formula of choline and propargylcholine. (*C*) Schematic representation of the synthesis of phosphatidyl-propargylcholine, followed by labeling with click reaction. (*D*) Immunofluorescence of PC and NS5A in Huh 7.5 cells at 18 h after HCV infection (MOI 3). Growth medium was supplemented with 100 μM of propargyl-choline at 17 hpi and incubated for 1 h. Propargyl-choline–labeled PCs and HCV NS5A protein were detected by Alexa Fluor 488–conjugated azide and anti-HCV NS5A mAb (9E10, IgG), respectively. Nuclei were stained with DAPI. Images are z-projection of 3D images. (*E*) Quantitation of the newly synthesized PC signal intensity per cell from multiple images in mock- and HCV-infected Huh-7.5 cells. (*F*) Mander's coefficient of colocalization showing the colocalized red and green pixels of NS5A and PC, as analyzed by JaCoP software. All the data represent the mean ± SD from three biological replicates. n denotes the number of cells from three independent biological experiments.

probed with antibodies to CCTα and NS5A. In mock-infected cells, CCTα was predominantly nuclear, whereas in HCV-infected cells, it was enriched in the perinuclear region and colocalized with the viral protein NS5A. Determination of the cytoplasmic to nuclear ratio (C/N) for HCV-infected samples indicated a value of approximately 2, significantly greater than that in mock cells, implying that HCV infection relocalizes CCTα from the nucleus to the cytosol near HCV replication sites (Fig. 2 *A*–*C*).

We also examined the expression of CCTα and observed a 2- to 4-fold increase in CCTα mRNA and protein expression at 18 and 24 h postinfection (Fig. 2 *D* and *E*). Further, to confirm the relocalization of CCTα, we fractionated mock- and HCV-infected

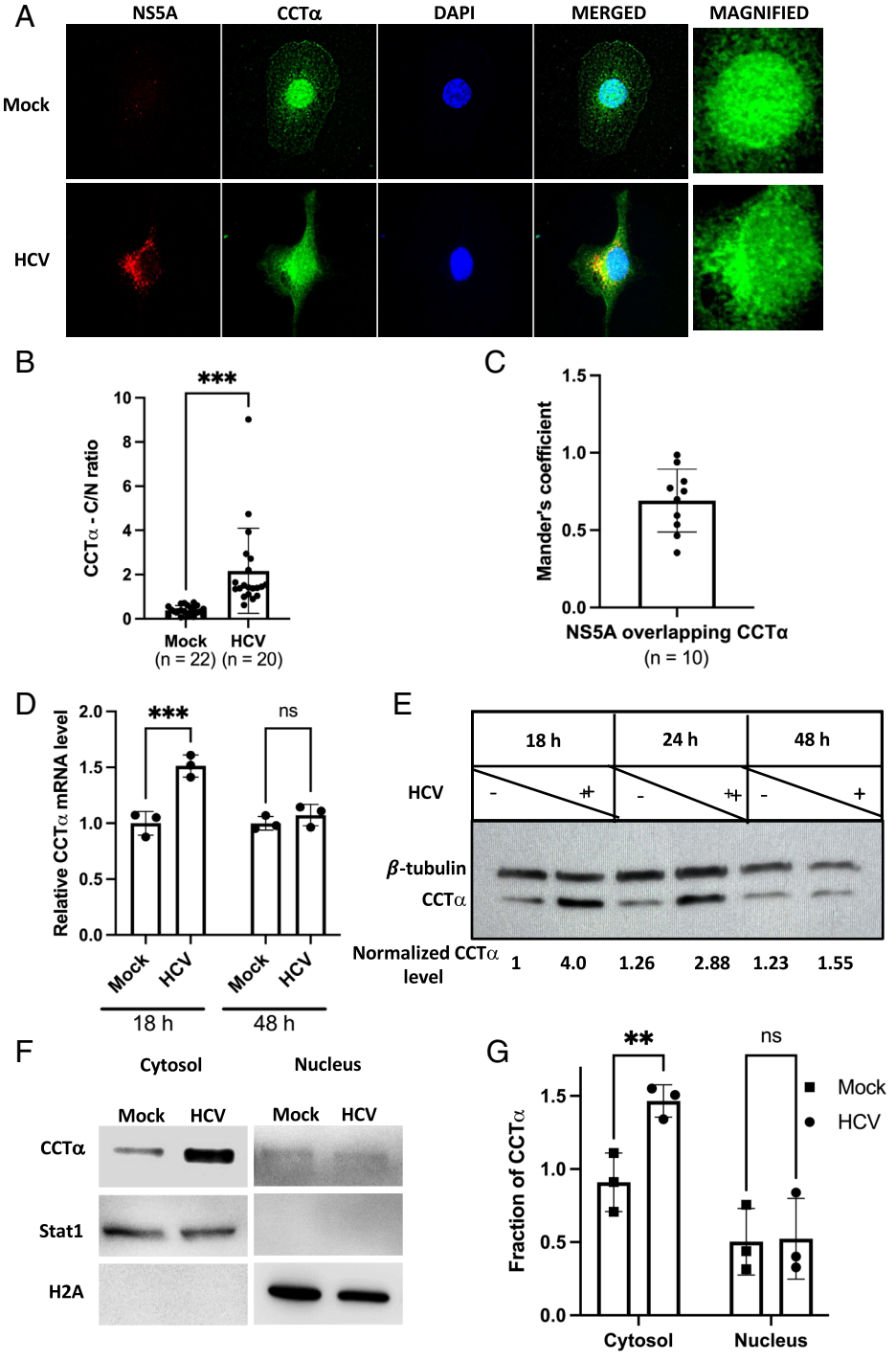

Fig. 2. HCV infection hijacks the Kennedy pathway. (*A*) Confocal imaging of CCTα and NS5A proteins in mock- and HCV-infected Huh 7.5 cells at 18 hpi. (*B*) The ratio of CCTα intensity in the cytoplasm to that in the nucleus of the mock- and HCV-infected cells was calculated from random fields of view. (*C*) Mander's coefficient of colocalization showing the colocalized red and green pixels of NS5A and CCTα, identified with JaCoP software. (*D*) Bar graphs demonstrating fold-change of CCTα mRNA level by quantitative RT-PCR, normalized against 18S rRNA, in mock- and HCV-infected Huh 7.5 cells at different time points. (*E*) Immunoblot of CCTα and β-tubulin protein from the whole cell lysates of mock- and HCV-infected Huh7.5 cells. Normalized CCTα protein level against b-tubulin protein is indicated at the bottom of their respective lanes. (*F*) Immunoblot showing CCTα protein expression in the cytoplasm and nucleus fraction of the mock- and HCV-infected Huh7.5 cells at 18 hpi. Stat1 and H2A were used to confirm equal loading of cytoplasm and nuclear extract proteins, respectively. (*G*) Quantitation of the CCTα protein level from panel Fig. 2*F*, normalized against respective loading controls. All the data represent the mean ± SD from three biological replicates, and n denotes the number of cells from three independent biological experiments.

cells at 18 hpi into their nuclear and cytoplasmic compartments and checked for the abundance of CCTα through immunoblotting. It was observed that the cytosolic fraction of HCV-infected cells had an elevated level of CCTα protein compared to mock, whereas no significant difference was observed in the nucleus fraction (Fig. 2 *F* and *G*). These data primarily suggest that to cope up with the PC demand during HCV infection, expression of the rate-limiting enzyme of the Kennedy pathway is stimulated.

CCTα Is Recruited to the Viral Replication Site for PC Synthesis. HCV RNA replication occurs within DMVs that are mainly derived from the ER membrane, with 50% of the DMVs remaining attached to the ER membrane (13, 34). To determine the association of CCTα with the HCV-induced membranous compartments during HCV replication, we performed membrane flotation assays (35) in naïve or Huh7.5 cells containing HCV subgenomic replicon (sg-Replicon). The fractions obtained were categorized as lipid droplet (LD)-rich and ER/endosome-rich based on the presence of different organelle-specific markers. In naïve Huh7.5 cells, CCTα was found to be distributed in both the fractions. However, in sg-Replicon cells, CCTα was significantly enriched in the ER/endosome-rich fraction, with a concentration approximately two-fold higher. In contrast, the subcellular distributions of LD- and ER-specific markers, ADRP and calnexin, did not change significantly upon HCV RNA replication (Fig. 3 *A* and *B*).

Next, we quantified the PC level in the crude ER fractions of naïve Huh 7.5 cells and sg-Replicon cells using a PC assay kit that utilizes phospholipase D to cleave choline from PC. The released choline oxidizes the OxiRed probe, producing fluorescence that was quantified (Ex/Em 535 nm/587 nm) (Abcam, ab83377). Consistent with our previous data, we observed an increase in PC level in cells engaged in active replication (Fig. 3*C*). The distribution of CCTα together with the enhancement of PC suggests that HCV replication mimics the condition that occurs during membrane biogenesis and indicates the involvement of CCTα-directed PC synthesis at HCV replication sites.

To further confirm whether CCTα is recruited to RCs, we examined the localization of CCTα with respect to markers involved in different phases of the HCV life cycle, such as NS5A (a multifunctional protein involved in both viral RNA replication and infectious virus assembly) (36), dsRNA (the HCV replication intermediate and a marker of viral RCs) (37), core protein (38), and lipid droplet (39) (both associated with HCV virion assembly). The Manders overlap coefficient analysis of CCTα colocalization with each of these proteins suggested that it colocalized more significantly with dsRNA (0.92) and NS5A (0.852) than with core (0.136) and LD (0.249) particle (Fig. 4). All these findings provide evidence that in cells involved with active HCV replication, CCTα membrane association is enhanced, with enrichment in ER/endosome-rich membranes, as defined by cofractionation and colocalization with NS5A and dsRNA, respectively. Hence, we conclude that CCTα is relocalized to the sites of active HCV replication.

CCTα Is Critical for PC Synthesis and HCV Replication. Next, we investigated the effects of depleting CCTα protein on HCV replication. We reduced the expression of CCTα in Huh 7.5 cells using lentivirus expressing shRNA against CCTα. The cells were subsequently infected with J6/JFH-1 HCV, and viral RNA, intra- and extracellular infectious virus, and specific infectivity were quantified 48 h postinfection. Immunoblot analysis confirmed efficient reduction of endogenous CCTα protein levels in cells expressing CCTα shRNA, compared to WT (Fig. 5*A*). We found that knockdown of CCTα significantly attenuated HCV RNA replication in CCTα KD cells by 1-log relative to control cells (Fig. 5*B*). Additionally, there was a significant 1-log reduction in infectious extracellular (Fig. 5*C*) and intracellular virus (Fig. 5*D*) production in HCV-infected cells. Specific infectivity was modestly decreased in the CCTα KD cells, indicating a possible secondary effect on virion lipid composition and infectivity (Fig. 5*E*). These findings define a significant role of CCTα in HCV RNA replication.

We further validated the role of CCTα in HCV replication by reducing the expression of CCTα, followed by transduction with a CCTα expression construct, which consists of modified shRNA target site and is thus resistant to shRNA-mediated silencing. We observed similar results, demonstrating that HCV replication was abrogated in CCTα-KD cells, while KD cells

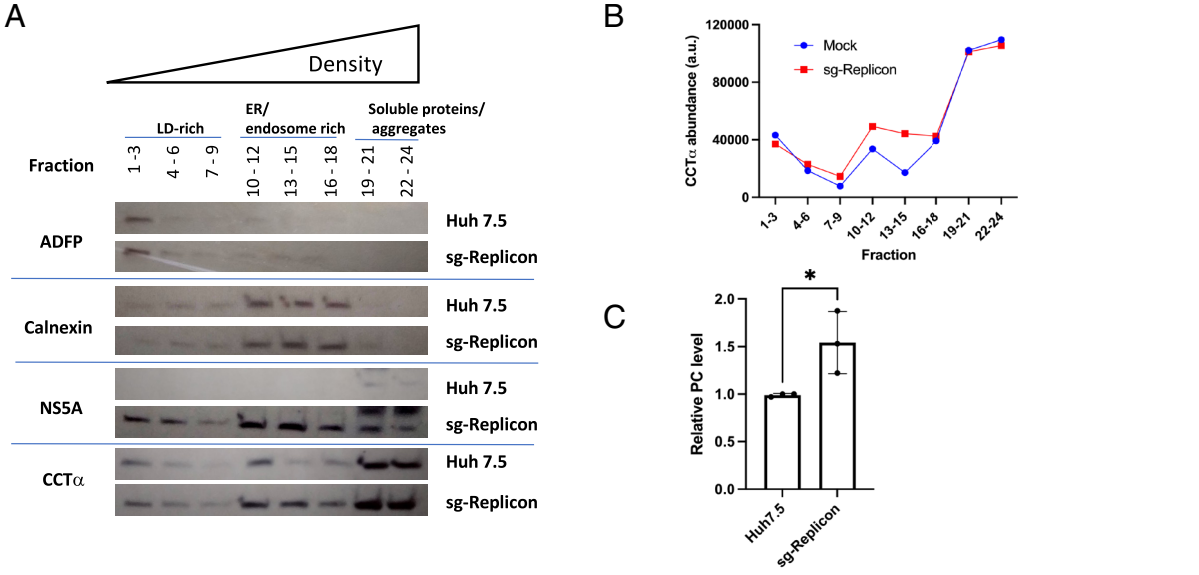

Fig. 3. CCTα cofractionates with HCV nonstructural protein NS5a during active HCV replication. (*A*) Immunoblot of the fractions collected following the membrane flotation assay in an iodixanol gradient of the naïve Huh 7.5 cells or Huh 7.5 cells harboring HCV-subgenomic replicon (sg-Replicon). Antibodies specific for calnexin, ADRP, NS5A, and CCT are used. (*B*) Profile of CCTα protein expression from western blot in (*A*). Protein quantification was done in Image]. (*C*) Quantitation of PC performed in the crude ER fraction of naïve Huh7.5 or Huh 7.5 cells harboring sg-Replicon using the manufacturer's protocol (Phosphatidylcholine Assay Kit, ab83377). All the data represent the mean ± SD from three independent biological replicates.

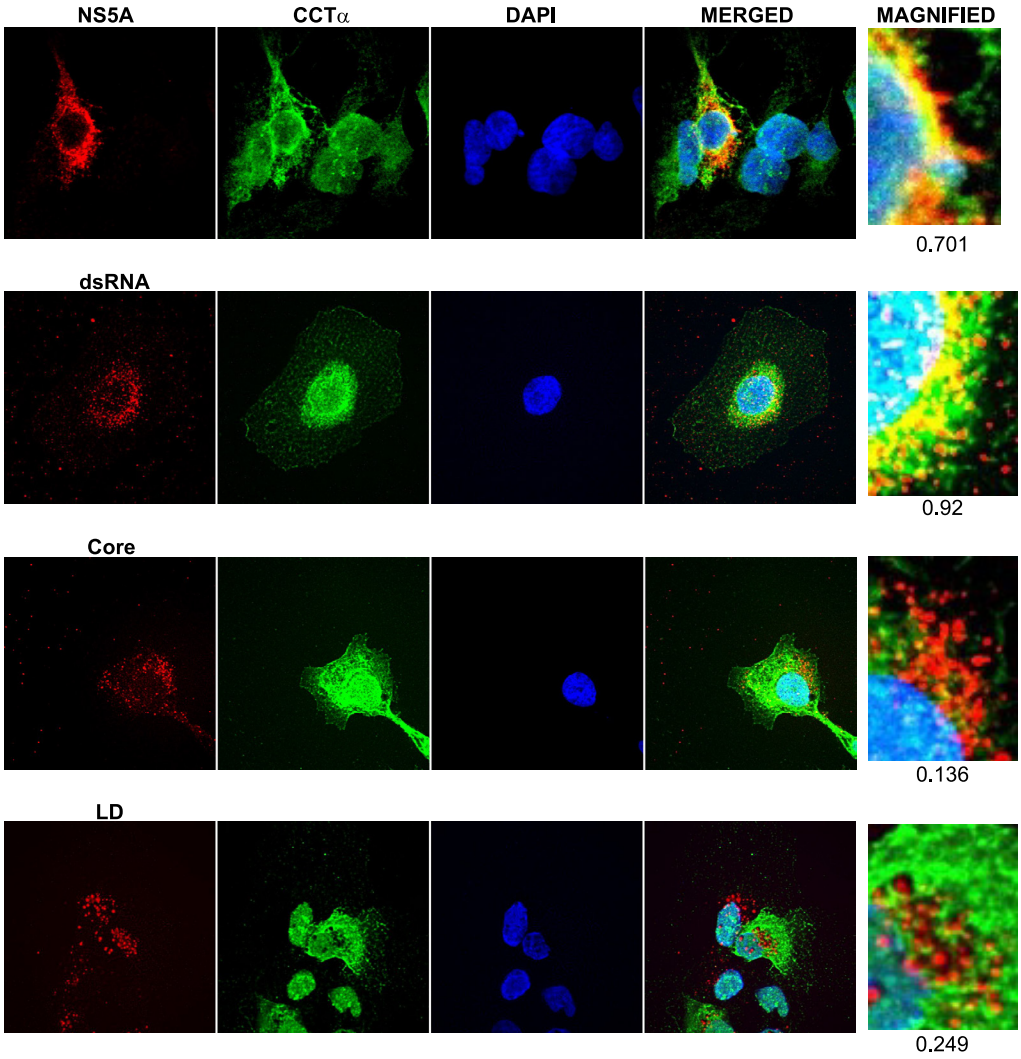

Fig. 4. HCV infection relocalizes CCTα to its active replication site. Indirect immunofluorescence of CCTα and NS5A/dsRNA/core/LD in HCV-infected Huh 7.5 cells at 18 hpi. Mander's coefficient of colocalization showing the colocalized red and green pixels of NS5A/ dsRNA/core/LD and CCTα, as identified with JaCoP software, are indicated at the *Bottom* of each image panel.

complemented with WT CCTα were refractory to HCV replication (Fig. 6 *A* and *B*). To further confirm that CCTα directed PC synthesis during HCV replication, we quantified PC levels using click chemistry. We performed immunofluorescence staining of PC and HCV NS5A proteins in CCTα KD cells and KD cells that were transcomplemented for CCTα expression. We compared these results with the PC enhancement observed in WT Huh 7.5 cells upon HCV infection. Interestingly, we observed no increase in PC levels in HCV-infected CCTα KD cells compared to WT cells. However, the PC level increased significantly in HCV-infected CCTα KD cells that were transcomplemented with shRNA-resistant CCTα (Fig. 6 *C* and *D*). This provides further evidence that CCTα is necessary for induced PC synthesis during HCV replication.

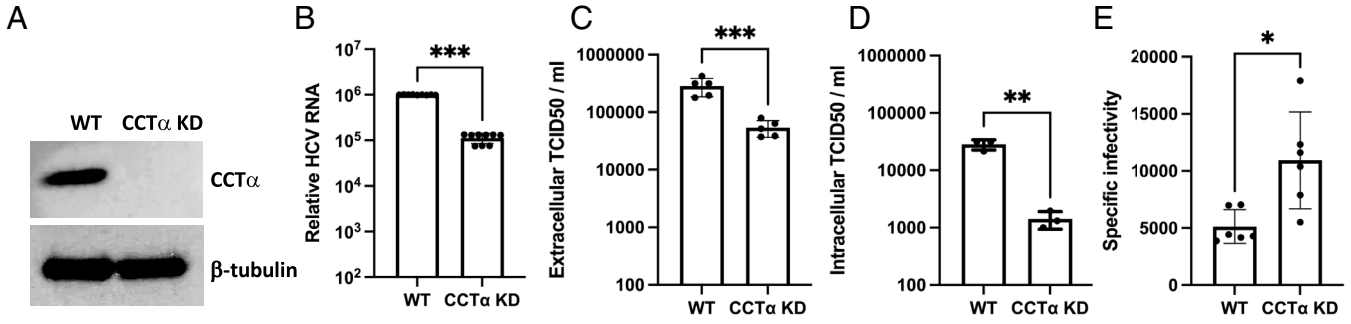

Fig. 5. CCTα is essential for HCV replication. (*A*) Immunoblot of CCTα in wild-type Huh 7.5 cells or Huh 7.5 cells stably expressing CCTα shRNA. b-tubulin is used as a loading control. (*B–E*) WT and CCTα KD- Huh 7.5 cells were infected with an MOI of 1 for 48 h followed by (*B*) quantitation of intracellular HCV RNA levels by real-time PCR and normalized to control values (18S rRNA) and (*C*) quantitation of extracellular and (*D*) intracellular infectious virions produced by calculating TCID50/ml. (*E*) Specific infectivity. All the data represent the mean ± SD from three independent biological replicates.

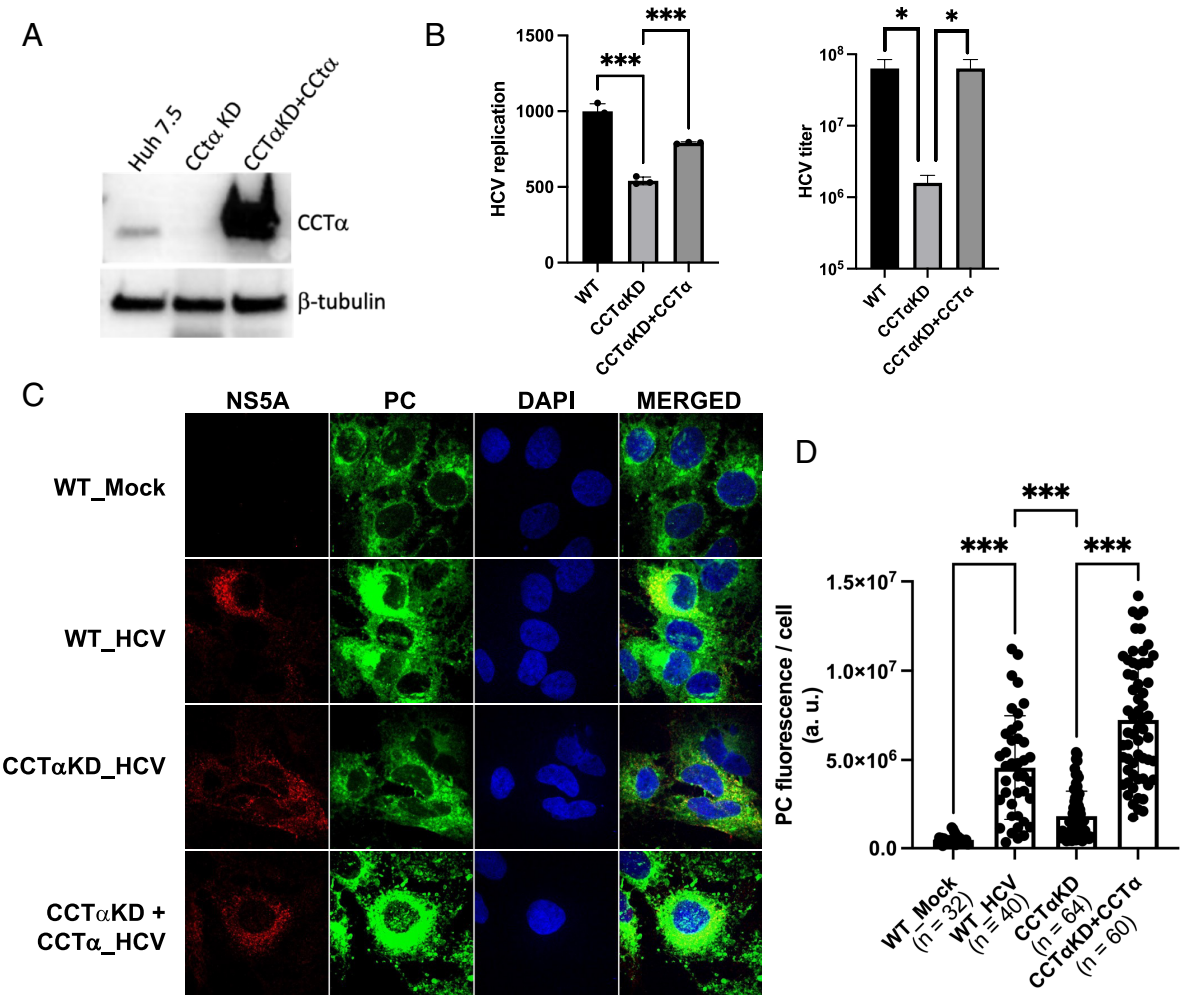

Fig. 6. CCTα-directed PC synthesis mediates HCV replication. (*A*) Immunoblot of CCTα in wild-type Huh 7.5 cells or Huh 7.5 cells stably expressing CCTα shRNA. b-tubulin is used as a loading control. (*B*) WT, CCTα KD-, and CCTα KD- cells expressing shRNA resistant CCTα plasmid cells were infected with an MOI of 1 for 96 h followed by quantitation of intracellular HCV RNA levels by real-time PCR and normalized to control values (18S rRNA) and quantitation of infectious virions produced by calculating TCID50/ml. (*C*) Immunofluorescence of PC and NS5A in WT or CCTα KD or transcomplemented CCTα KD Huh 7.5 cells at 24 hpi. (*D*) Quantitation of PC signal intensity per cell from multiple images in mock- and HCV-infected cells from panel *C*. All the data represent the mean ± SD from three biological replicates. n denotes the number of cells from three independent biological experiments.

NS3-4A Protease Activity Is Critical for Inducing De Novo PC Synthesis During HCV Infection. We then aimed to identify the specific HCV protein(s) responsible for modulating PC levels in the cells. We utilized U2OS cell lines that express individual genotype 1a HCV proteins or the entire polyprotein (UHCV) upon induction by removing tetracycline from the cell culture media. These cell lines are well-established models for studying HCV gene expression and RC formation, allowing us to study HCV-induced membranous web formation without interference from viral entry, assembly, or egress (40, 41). Specifically, we examined UHCVcon-57.3 cells which express the entire ORF, UNS3-4A-24 cells, which express the NS3-4A complex, and UNS5Acon-37.2 cells, which express the NS5A protein in a tightly regulated manner. Using click chemistry followed by immunofluorescence, we observed an enhanced PC signal in induced UHCVcon-57.3 cells and UNS3-4A-24 cells compared to their respective uninduced counterparts. However, no enhanced PC signal was detected in induced UNS5Acon-37.2 cells (Fig. 7). This suggests that the expression of NS3-4A is sufficient to induce PC synthesis.

NS3 possesses helicase and serine protease activities, while NS4A acts as a cofactor. To test the essential role of protease activity of NS3 in this process, we chemically perturbed its activity using telaprevir (42), an FDA-approved NS3-4A protease inhibitor. We evaluated PC synthesis and CCTα relocalization through immunofluorescence. Strikingly, we observed that neither PC signal was enhanced in cells induced to express NS3-4A proteins in the presence of telaprevir, nor was there relocalization of CCTα from the nucleus to the ER membrane (Fig. 8). This strongly concludes that the protease activity of NS3 is crucial in modulating the Kennedy pathway for HCV-mediated de novo synthesis of PC in UNS3-4A-24 cells.

Discussion

Our study elucidates the mechanisms by which HCV manipulates host lipid metabolism, specifically PC metabolism, to facilitate its replication. We demonstrated that HCV infection relocalizes CCTα to RCs, inducing de novo PC synthesis at the replication site. Our findings also highlight the crucial role of the HCV NS3-4A protease in orchestrating de novo PC synthesis by hijacking the Kennedy pathway. This finding extends our understanding of the molecular mechanisms that HCV employs to create a favorable lipid niche for its replication inside the host cells and emphasizes the importance of spatial specificity of lipid synthesis during viral replication.

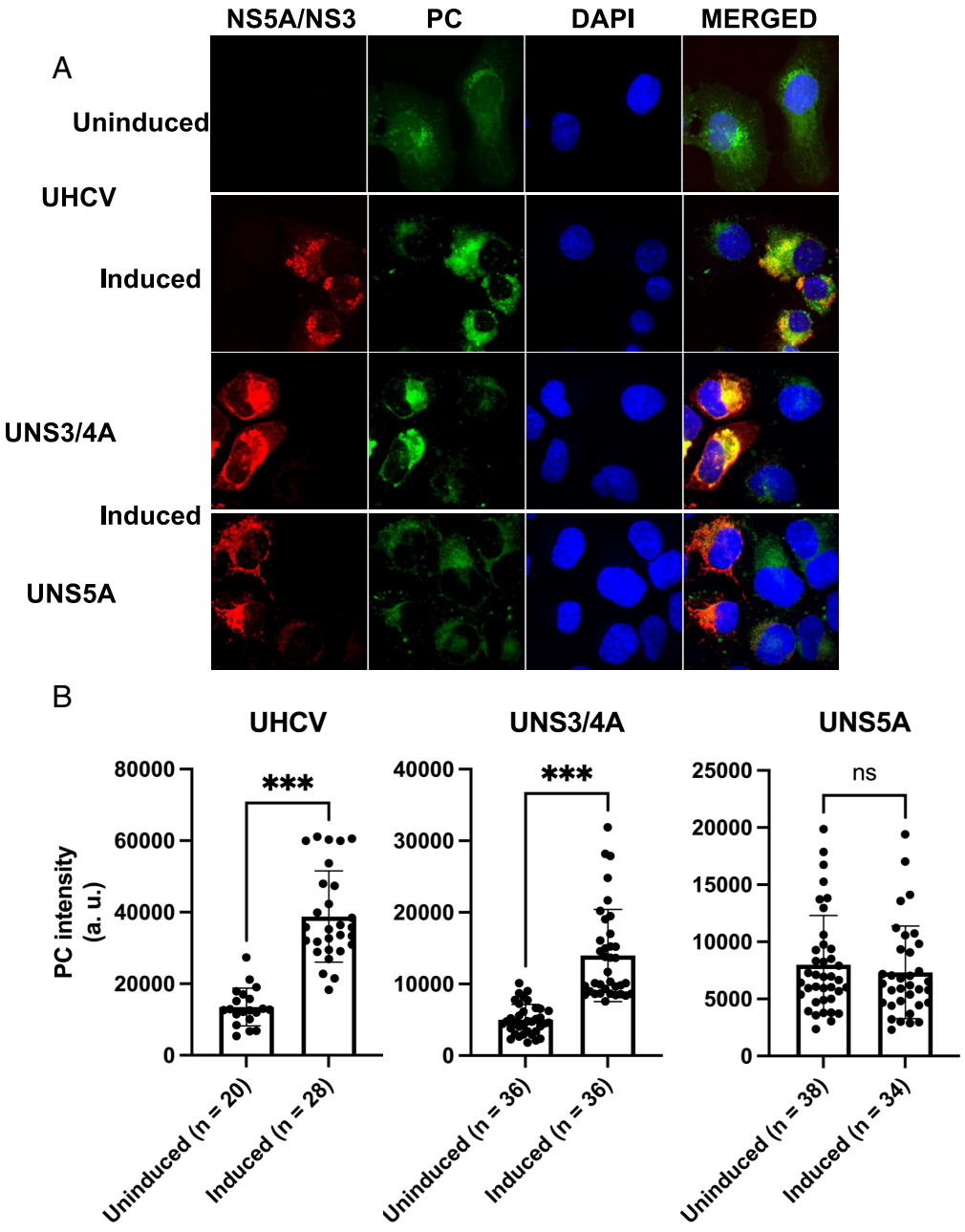

Fig. 7. HCV NS3/4A protease is essential for inducing PC synthesis. (*A*) Immunofluorescence of PC and NS3/NS5A in U2OS osteosarcoma UHCV (polyprotein), UNS5A, and UNS5B cell lines grown in either uninduced conditions (*Top* panel) or induced expression conditions (the other three panels) and imaged 24 h postinduction. (*B*) Bar graph showing the newly synthesized PC signal intensity per cell from multiple images in panel A. All the data represent the mean ± SD from three biological replicates. n denotes the number of cells from three independent biological experiments.

Comparative studies with other positive-strand RNA viruses highlight the significance of PC synthesis at the viral replication sites. For instance, Zhang et al. showed that brome mosaic virus (BMV) increases PC content at its replication sites by recruiting the host enzyme Cho2p, critical for PC synthesis, to the viral replication complexes (VRCs) (24). This finding is consistent with our observation of enhanced PC synthesis in HCV-infected cells, suggesting a conserved strategy among positive-strand RNA viruses to manipulate host lipid metabolism for efficient replication. Another study on FHV found that FHV RNA replication in Drosophila cells is associated with increased PC accumulation, highlighting the role of specific lipid metabolism pathways in viral replication (43). Similarly, Xu and Nagy demonstrated that Tomato bushy stunt virus (TBSV) replication requires phosphatidylethanolamine (PE)-enriched membrane microdomains, highlighting the importance of membrane lipid composition in the replication of positive-strand RNA viruses (44). These insights collectively advance our understanding of the complex interplay between viral proteins and host lipid metabolism, offering a broader perspective on how positive-strand RNA viruses exploit host cellular machinery. Targeting these lipid biosynthesis pathways represents a promising approach for developing broad-spectrum antiviral therapies that could potentially mitigate the replication of diverse viruses within this group.

One of the key findings in our study is the relocation of CCTα, the rate-limiting enzyme in the Kennedy pathway of PC synthesis. HCV infection triggers the translocation of CCTα from the nucleus to the replication sites, specifically DMVs. This relocalization is crucial for meeting the elevated PC demand during viral replication. The increased expression and redistribution of CCTα, coupled with elevated PC levels at replication sites, suggest that HCV effectively hijacks the host's lipid biosynthesis machinery to ensure an early infection supply of membrane components essential for its replication.

The other most conceptually innovative aspect of this study is the requirement of the viral protease activity of NS3/4A. NS3/4A is a key component of the viral replication complex, known for

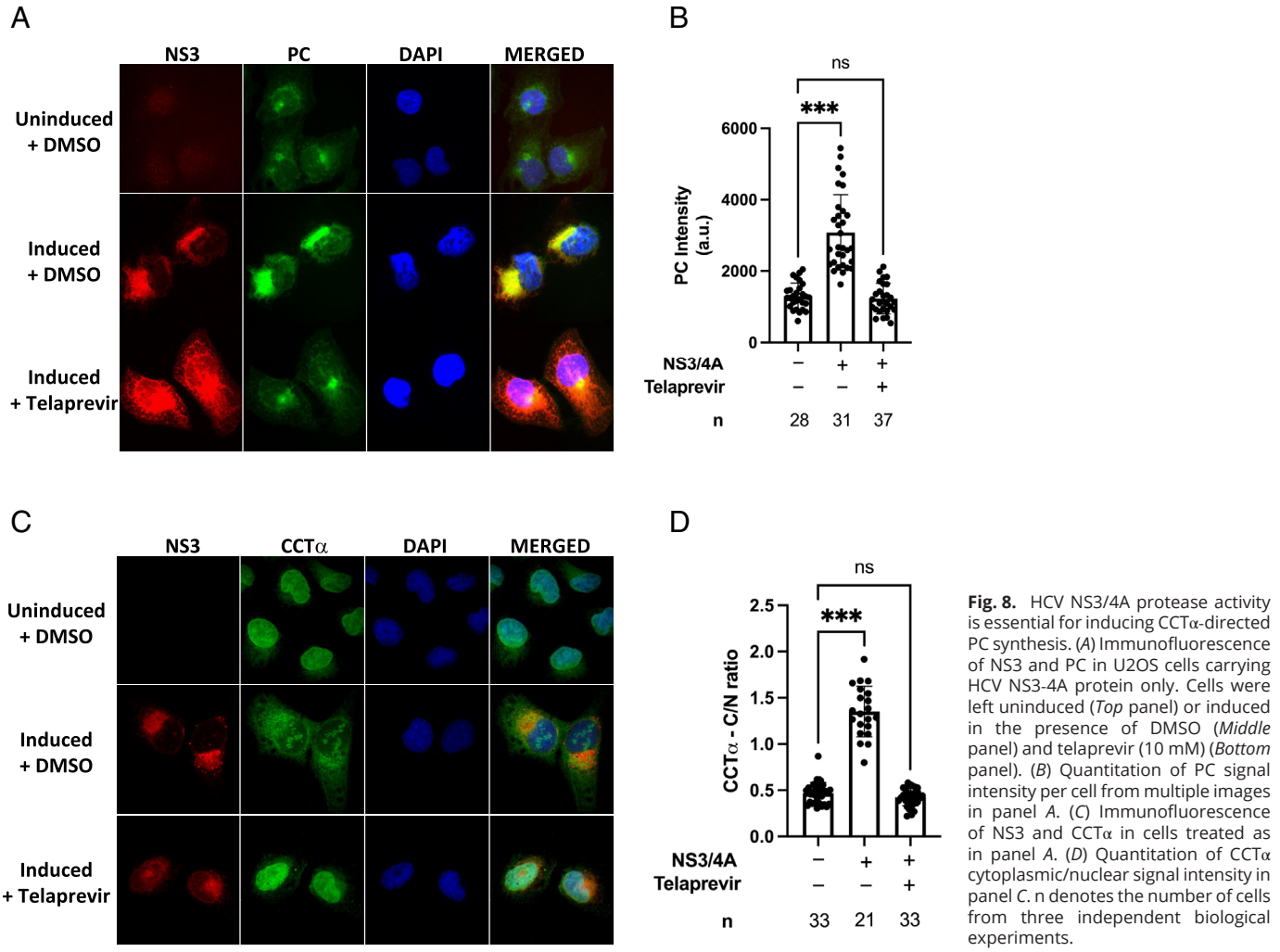

Fig. 8. HCV NS3/4A protease activity is essential for inducing CCTα-directed PC synthesis. (*A*) Immunofluorescence of NS3 and PC in U2OS cells carrying HCV NS3-4A protein only. Cells were left uninduced (*Top* panel) or induced in the presence of DMSO (*Middle* panel) and telaprevir (10 mM) (*Bottom* panel). (*B*) Quantitation of PC signal intensity per cell from multiple images in panel *A*. (*C*) Immunofluorescence of NS3 and CCTα in cells treated as in panel *A*. (*D*) Quantitation of CCTα cytoplasmic/nuclear signal intensity in panel *C*. n denotes the number of cells from three independent biological experiments.

cleaving and inactivating host factors. This activity disrupts host antiviral defenses, thereby facilitating viral persistence (45–50). We identified that NS3-4A directly or indirectly influences CCTα's relocalization. The inhibition of NS3-4A protease activity using telaprevir abrogated this effect, suggesting the protease's essential role in this process. Interestingly, picornavirus modulation of PC synthesis requires the unrelated viral protease 2A (mechanism unknown) (51). Thus, picornaviruses and HCV may have converged evolutionarily on a common protease-dependent strategy. Additionally, the HCV NS3-4A protease also modulates the host lipid environment by cleaving 24-dehydrocholesterol reductase (DHCR24), an enzyme critical for cholesterol biosynthesis. As described by Tallorin et al., NS3-4A protease cleaves DHCR24 between residues Cys91 and Thr92, leading to the accumulation of desmosterol, an immediate precursor to cholesterol. This cleavage results in reduced conversion of desmosterol to cholesterol, increasing membrane fluidity at replication sites, which is beneficial for viral RNA replication (52). This dual role of NS3-4A in modulating both PC and desmosterol synthesis highlights its central role in creating a favorable lipid environment for HCV replication.

In conclusion, this study identifies a role for NS3/4A in modulating the Kennedy pathway to stimulate PC synthesis at RCs. Future studies will focus on identifying the molecular target of the protease. These insights not only enhance our understanding of HCV biology but also pave the way for developing antiviral therapies targeting lipid metabolic pathways.

Materials and Methods

Labeling of Newly Synthesized PC via Click Chemistry. At 16 hpi, Huh 7.5 cells were rinsed with PBS and incubated for 1 h in serum-free media at 37 °C. After depriving cells of serum for 1 h, 100uM propargylcholine (Aobious, AOBT7378) was added into the media, and cells were incubated for another 1 h at 37 °C, followed by fixation with 4% paraformaldehyde in PBS for 10 min. Subsequently, incorporated propargylcholine was stained with Alexa 488 azide (Molecular Probes™, A10266) by using the click chemistry method following the Click-iT Cell Reaction Buffer Kit protocol (Invitrogen, C10269).

Immunofluorescence. Cells grown on a coverslip in 24-well plates were either infected with HCV or induced to express HCV proteins for the indicated time, fixed with 4% formaldehyde in PBS for 10 min, and washed for 3 times with PBS. To detect CCTα immunostaining, cells were permeabilized with 0.1% Triton X-100 for 10 min, followed by blocking with 10% goat serum for 1 h. For staining other proteins, cells were incubated with 10% goat serum along with 0.05% saponin for 1 h. Following blocking and permeabilizing, cells were stained overnight with primary antibodies in blocking buffer at 4 °C. Subsequently, cells were washed 3 times with PBS, followed by incubation with secondary antibody for 1 h. After several washes, coverslips were mounted in ProLong Gold AntiFade with DAPI (4′,6′-diamidino-2-phenylindole) nuclear stain (Invitrogen). The samples were imaged using an Olympus DSU spinning disc confocal microscope, and images were taken using Slidebook v6.0 software and processed using ImageJ (NIH). Quantification of fluorescence intensity was determined from multiple images taken from triplicate coverslips using ImageJ.

HCV Quantification. Virus titers were determined by analyzing a limiting dilution assay for NS5A expression as described (53). Viral RNA was quantified by real-time RT-PCR analysis using the NucleoSpin 96 RNA kit per the manufacturer's

instructions. Eluted RNAs were reverse transcribed and PCR amplified for HCV NS4B and 18S rRNA using the Superscript III Platinum one-step RT–PCR system with Platinum Taq (Life Technologies) as described (54). 18S rRNA served as an internal control and was used to normalize the data. Relative quantitation was calculated using the standard curve method.

Membrane Flotation Assay. Membrane flotation was performed as previously described by Vogt et al. (35). Briefly. Huh 7.5 cells or Huh 7. 5 cells carrying HCV subgenomic replicon were washed, scraped, and counted. An equal number of cells for each sample were resuspended in 1.5 ml PBS containing 0.25 M sucrose and lysed using a tight-fitting Dounce homogenizer (Wheaton). The cell lysate was cleared of cellular debris and nuclei by spinning at 2500×*g* for 10 min at 4 °C. 7 mg of the cleared lysate for each sample was mixed with an equal volume of 60% iodixanol (Sigma) such that it resulted in a 30% iodixanol concentration and poured at the bottom of the tube. Then, a discontinuous iodixanol gradient was prepared by layering 20 and 10% iodixanol on top of it. The 30–20–10% iodixanol gradient was then spun at 30,000 rpm for 16 h at 4 °C in a SW41T Rotor. 22 fractions were collected from top to bottom, and samples were analyzed by performing immunoblot using different antibodies. Quantification of protein expression was done in ImageJ Software.

Data, Materials, and Software Availability. All data in this manuscript data have been deposited in Mendeley Data (https://doi.org/10.17632/g3yhhf-ht2t.1) (55).

ACKNOWLEDGMENTS. We thank Charles Rice and Arash Grakoui for providing reagents. This work was funded by R01AI137514 and R01AI173337 to G.R. and an American Heart Association postdoctoral fellowship to S.S.

1. P. Axley, Z. Ahmed, S. Ravi, A. K. Singal, Hepatitis C virus and hepatocellular carcinoma: A narrative review. *J. Clin. Transl. Hepatol.* **6**, 79–84 (2018).
2. E. Gower, C. Estes, S. Blach, K. Razavi-Shearer, H. Razavi, Global epidemiology and genotype distribution of the hepatitis C virus infection. *J. Hepatol.* **61**, S45–S57 (2014).
3. World Health Organization, Global hepatitis report (2017), https://www.who.int/hepatitis/publications/global-hepatitis-report2017/en/.
4. G. H. Syed, Y. Amako, A. Siddiqui, Hepatitis C virus hijacks host lipid metabolism. *Trends Endocrinol. Metab* **21**, 33 (2010).
5. M. F. Bassendine *et al.*, HCV and the hepatic lipid pathway as a potential treatment target. *J. Hepatol.* **55**, 1428–1440 (2011).
6. S. Miller, J. Krijnse-Locker, Modification of intracellular membrane structures for virus replication. *Nat. Rev. Microbiol.* **6**, 363–374 (2008).
7. A. Shulla, G. Randall, (+) RNA virus replication compartments: A safe home for (most) viral replication *Curr. Opin. Microbiol.* **32**, 82–82 (2016).
8. S. Welsch *et al.*, Composition and three-dimensional architecture of the dengue virus replication and assembly sites. *Cell Host Microbe* **5**, 365–375 (2009).
9. L. K. Gillespie, A. Hoenen, G. Morgan, J. M. Mackenzie, The endoplasmic reticulum provides the membrane platform for biogenesis of the flavivirus replication complex. *J. Virol.* **84**, 10438–10447 (2010).
10. B. G. Kopek, G. Perkins, D. J. Miller, M. H. Ellisman, P. Ahlquist, Three-dimensional analysis of a viral RNA replication complex reveals a virus-induced mini-organelle. *PLoS Biol* **5**, e220 (2007).
11. P. M. Grimley, I. K. Berezesky, R. M. Friedman, Cytoplasmic structures associated with an arbovirus infection: Loci of viral ribonucleic acid synthesis. *J. Virol.* **2**, 1326–1338 (1968).
12. P. Kujala *et al.*, Biogenesis of the Semliki Forest virus RNA replication complex. *J. Virol.* **75**, 3873–3884 (2001).
13. I. Romero-Brey *et al.*, Three-dimensional architecture and biogenesis of membrane structures associated with hepatitis C virus replication. *PLoS Pathog* **8**, e1003056 (2012).
14. G. Wolff, C. E. Melia, E. J. Snijder, M. Bárcena, Double-membrane vesicles as platforms for viral replication. *Trends Microbiol.* **28**, 1022–1033 (2020).
15. D. Egger *et al.*, Expression of hepatitis C virus proteins induces distinct membrane alterations including a candidate viral replication complex. *J. Virol.* **76**, 5974–5984 (2002).
16. V. Lohmann *et al.*, Replication of subgenomic hepatitis C virus RNAs in a hepatoma cell line. *Science* **285**, 110–113 (1999).
17. D. Paul, R. Bartenschlager, Flaviviridae replication organelles: Oh, what a tangled web we weave. *Annu. Rev. Virol.* **2**, 289–310 (2015).
18. K. L. Berger *et al.*, Roles for endocytic trafficking and phosphatidylinositol 4-kinase III alpha in hepatitis C virus replication. *Proc. Natl. Acad. Sci. U.S.A.* **106**, 7577–7582 (2009).
19. S. Reiss *et al.*, Recruitment and activation of a lipid kinase by hepatitis C virus NS5A is essential for integrity of the membranous replication compartment. *Cell Host Microbe* **9**, 32–45 (2011).
20. H. Wang *et al.*, Oxysterol-binding protein is a phosphatidylinositol 4-kinase effector required for HCV replication membrane integrity and cholesterol trafficking. *Gastroenterology* **146**, 1373–1385.e11 (2014).
21. D. L. Diamond *et al.*, Temporal proteome and lipidome profiles reveal hepatitis C virus-associated reprogramming of hepatocellular metabolism and bioenergetics. *PLoS Pathog* **6**, e1000719 (2010).
22. S. Hofmann *et al.*, Complex lipid metabolic remodeling is required for efficient hepatitis C virus replication. *Biochim. Biophys. Acta Mol. Cell Biol. Lipids* **1863**, 1041–1056 (2018).
23. B. Roe, E. Kensicki, R. Mohney, W. W. Hall, Metabolomic profile of hepatitis C virus-infected hepatocytes. *PLoS One*. **6**, e23641 (2011). Available from: https://www.ncbi.nlm.nih.gov/pmc/articles/PMC3154941/
24. J. Zhang *et al.*, Positive-strand RNA viruses stimulate host phosphatidylcholine synthesis at viral replication sites. *Proc. Natl. Acad. Sci. U.S.A.* **113**, E1064–E1073 (2016).
25. G. van Meer, D. R. Voelker, G. W. Feigenson, Membrane lipids: Where they are and how they behave. *Nat. Rev. Mol. Cell Biol.* **9**, 112 (2008).
26. S. A. Henry, S. D. Kohlwein, G. M. Carman, Metabolism and regulation of glycerolipids in the yeast Saccharomyces cerevisiae. *Genetics* **190**, 317–349 (2012).
27. V. V. Rostovtsev, L. G. Green, V. V. Fokin, K. B. Sharpless, A stepwise Huisgen cycloaddition process: Copper(I)-catalyzed regioselective "ligation" of azides and terminal alkynes. *Angew Chem. Int. Ed Engl.* **41**, 2596–2599 (2002).
28. C. W. Tornøe, C. Christensen, M. Meldal, Peptidotriazoles on solid phase: [1,2,3]-triazoles by regiospecific copper(i)-catalyzed 1,3-dipolar cycloadditions of terminal alkynes to azides. *J. Org. Chem.* **67**, 3057–3064 (2002).
29. C. Y. Jao, M. Roth, R. Welti, A. Salic, Metabolic labeling and direct imaging of choline phospholipids in vivo. *Proc. Natl. Acad. Sci. U.S.A.* **106**, 15332–15337 (2009).
30. M. Tavasoli, S. Lahire, T. Reid, M. Brodovsky, C. R. McMaster, Genetic diseases of the Kennedy pathways for membrane synthesis. *J. Biol. Chem.* **295**, 17877–17886 (2020).
31. C. J. DeLong, Y. J. Shen, M. J. Thomas, Z. Cui, Molecular distinction of phosphatidylcholine synthesis between the CDP-choline pathway and phosphatidylethanolamine methylation pathway. *J. Biol. Chem.* **274**, 29683–29688 (1999).
32. C. Kent, CTP:Phosphocholine cytidylyltransferase. *Biochim. Biophys. Acta Lipids Lipid Metab.* **1348**, 79–90 (1997).
33. R. B. Cornell, N. D. Ridgway, CTP:Phosphocholine cytidylyltransferase: Function, regulation, and structure of an amphitropic enzyme required for membrane biogenesis. *Prog. Lipid Res.* **59**, 147–171 (2015).
34. P. Ferraris, E. Blanchard, P. Roingeard, Ultrastructural and biochemical analyses of hepatitis C virus-associated host cell membranes. *J. Gen. Virol.* **91**, 2230–2237 (2010).
35. D. A. Vogt *et al.*, Lipid droplet-binding protein TIP47 regulates hepatitis C virus RNA replication through interaction with the viral NS5A protein. *PLoS Pathog.* **9**, e1003302 (2013).
36. D. Paul, V. Madan, R. Bartenschlager, Hepatitis C virus RNA replication and assembly: Living on the fat of the land. *Cell Host Microbe* **16**, 569–579 (2014).
37. P. Targett-Adams, S. Boulant, J. McLauchlan, Visualization of double-stranded RNA in cells supporting hepatitis C virus RNA replication. *J. Virol.* **82**, 2182–2195 (2008), https://journals.asm.org/doi/abs/10.1128/JVI.01565-07.
38. N. A. Counihan, S. M. Rawlinson, B. D. Lindenbach, Trafficking of hepatitis C virus core protein during virus particle assembly. *PLoS Pathog.* **7**, e1002302 (2011).
39. Y. Miyanari *et al.*, The lipid droplet is an important organelle for hepatitis C virus production. *Nat. Cell Biol.* **9**, 1089–1097 (2007).
40. D. Moradpour, P. Kary, C. M. Rice, H. E. Blum, Continuous human cell lines inducibly expressing hepatitis C virus structural and nonstructural proteins. *Hepatology* **28**, 192–201 (1998).
41. R. Gosert *et al.*, Identification of the hepatitis C virus RNA replication complex in Huh-7 cells harboring subgenomic replicons. *J. Virol.* **77**, 5487–5492 (2003).
42. A. D. Kwong, R. S. Kauffman, P. Hurter, P. Mueller, Discovery and development of telaprevir: An NS3-4A protease inhibitor for treating genotype 1 chronic hepatitis C virus. *Nat. Biotechnol.* **29**, 993–1003 (2011).
43. K. M. Castorena, K. A. Stapleford, D. J. Miller, Complementary transcriptomic, lipidomic, and targeted functional genetic analyses in cultured Drosophila cells highlight the role of glycerophospholipid metabolism in Flock House virus RNA replication. *BMC Genomics* **11**, 183 (2010).
44. K. Xu, P. D. Nagy, RNA virus replication depends on enrichment of phosphatidylethanolamine at replication sites in subcellular membranes. *Proc. Natl. Acad. Sci. U.S.A.* **112**, E1782–E1791. Available from: https://pnas.org/doi/full/10.1073/pnas.1418971112
45. K. Li *et al.*, Immune evasion by hepatitis C virus NS3/4A protease-mediated cleavage of the Toll-like receptor 3 adaptor protein TRIF. *Proc. Natl. Acad. Sci. U.S.A.* **102**, 2992–2997 (2005).
46. E. Meylan *et al.*, Cardif is an adaptor protein in the RIG-I antiviral pathway and is targeted by hepatitis C virus. *Nature* **437**, 1167–1172 (2005).
47. X. Kang *et al.*, DDB1 is a cellular substrate of NS3/4A protease and required for hepatitis C virus replication. *Virology* **435**, 385–394 (2013).
48. K. Morikawa *et al.*, Quantitative proteomics identifies the membrane-associated peroxidase GPx8 as a cellular substrate of the hepatitis C virus NS3-4A protease. *Hepatology* **59**, 423–433 (2014).
49. B. Gagné, N. Tremblay, A. Y. Park, M. Baril, D. Lamarre, Importin β1 targeting by hepatitis C virus NS3/4A protein restricts IRF3 and NF-κB signaling of IFNB1 antiviral response. *Traffic* **18**, 362–377 (2017).
50. H. T. L. Tran *et al.*, OCIAD1 is a host mitochondrial substrate of the hepatitis C virus NS3-4A protease. *PLoS One* **15**, e0236447 (2020).
51. J. A. Nchoutmboube *et al.*, Increased long chain acyl-Coa synthetase activity and fatty acid import is linked to membrane synthesis for development of picornavirus replication organelles. *PLoS Pathog.* **9**, e1003401 (2013).
52. L. Tallorin *et al.*, Hepatitis C virus NS3-4A protease regulates the lipid environment for RNA replication by cleaving host enzyme 24-dehydrocholesterol reductase. *J. Biol. Chem.* **295**, 12426–12436 (2020).
53. B. D. Lindenbach *et al.*, Complete replication of hepatitis C virus in cell culture. *Science* **309**, 4 (2005).
54. T. E. Oakland, K. J. Haselton, G. Randall, EWSR1 binds the hepatitis C virus cis-acting replication element and is required for efficient viral replication. *J. Virol.* **87**, 6625–6634 (2013), https://journals.asm.org/doi/abs/10.1128/JVI.01006-12.
55. S. Sarwar, G. Randall, HCV NS3/4A protease induces CCTα relocalization to viral replication sites, stimulating phosphatidylcholine synthesis and promoting viral replication. Mendeley Data, V1. https://doi.org/10.17632/g3yhhfht2t.1. Deposited 17 February 2025.